Annual Cycle of Total Ozone Content in the Southern Hemisphere Using the Chemistry-Climate Model SOCOLv3

Vladimir Zubov *, Andrey Mironov, Tatiana Egorova, Eugene Rozanov *

Posted Date: 20 September 2023

doi: 10.20944/preprints202309.1348.v1

Keywords: ozone layer; chemistry-climate models; photolysis; horizontal transport

Article

Annual Cycle of Total Ozone Content in the Southern Hemisphere Using the Chemistry-Climate Model SOCOLv3

Vladimir Zubov [1,2,*], Andrey Mironov [1], Tatiana Egorova [3] and Eugene Rozanov [1,3]

[1] St. Petersburg State University, St. Petersburg, Russia; v_zubov@rambler.ru
[2] Voeikov Main Geophysical Observatory, St. Petersburg, Russia; v_zubov@rambler.ru
[3] Physikalisch-Meteorologisches Observatorium and World Radiation Center, Davos, Switzerland; t.egorova@pmodwrc.ch
* Correspondence: v_zubov@rambler.ru; Tel.: +7 (921) 189-64-06

Abstract: Several chemistry-climate models (CCM) underestimate the total column ozone (TCO) over the polar region in the Southern Hemisphere during wintertime. To evaluate potential causes of the problem, we exploit CCM SOCOLv3 to study the TCO over Antarctica sensitivity to the: (1) photo-dissociation rates of ozone for large solar zenith angles; (2) rates of the stratospheric heterogeneous reactions, and (3) intensity of the meridional flux into the polar regions due to sub-grid scale mixing processes in the model. Comparisons of the model results with the satellite-based IASI (Infrared Atmospheric Sounder Interferometer) sensor measurements showed that the most important processes for the improvement of the polar ozone simulation results are photolysis and horizontal mixing. The reasonable tuning of these factors has allowed us to improve the model representation of the ozone annual cycle over the southern polar region. The proposed increase of the horizontal mixing can be recommended for the CCMs with relatively low horizontal resolution.

Keywords: ozone layer; chemistry-climate models; photolysis; horizontal transport

1. Introduction

The atmospheric ozone (O_3) layer is an essential factor for the sustainability of the Earth's biosphere and human health. It protects all living beings from the Sun's harmful ultraviolet radiation in the UV-C and UV-B bands of the solar spectrum. Also, as a radiatively-active gas ozone contributes substantially to the energy balance of the atmosphere and underlying surface [1].

Caused by emissions of chlorine and bromine-containing substances, stratospheric ozone has been depleted since the 1970s. In the 1980s, decreasing the total column ozone (TCO) was detected in the middle latitudes of both hemispheres and the Antarctic ozone hole was discovered [2]. Governments around the world created an agreement to limit the production of chlorofluorocarbons (CFCs)—the Montreal Protocol, which came into force in 1989. To estimate the Protocol effectiveness and the atmospheric ozone evolution in the 21st century a special class of the models—Chemistry-Climate models (CCM) has been applied [3]. CCM considers the main processes responsible for the ozone layer state and allows one to calculate the base characteristics of the general circulation of the Earth's atmosphere [4–6].

Usually, the CCM performance over the high latitudes was estimated only for the periods when solar light is available and it was shown that many models possess a good performance over the southern high latitudes in early spring [6–8]. The lack of model validation during the polar night is because, until 2014 in the polar latitudes of the Southern Hemisphere, most satellite instruments could not measure the ozone due to the absence of solar illumination. The only TOVS (The TIROS Operational Vertical Sounder) satellite instrument performed measurements of TCO during the polar night, but its relative measurement error was too high [9]. The situation changed with the start of

Preprints (www.preprints.org) | NOT PEER-REVIEWED | Posted: 20 September 2023 doi:10.20944/preprints202309.1348.v1

ozone measurements using the IASI (Infrared Atmospheric Sounding Interferometer), which allows to obtain data on the ozone content at night and daytime conditions with an accuracy of 5% [10].

Figure 1 illustrates the climatological annual course of TCO (in Dobson Units or DU) averaged over 75-80°S from the satellite measurements with ISAI and SBUV sensors together with the results of SOCOLv3, CMAM, GEOSCCM, MRI-ESM, MIROC3.2, EMAC-L47MA, and NIWA-UKCA chemistry-climate models. SBUV data were acquired from https://acd-ext.gsfc.nasa.gov/Data_services/merged. The IASI data were downloaded from the instrument site (https://iasi.aeris-data.fr/). The model data were acquired from the CCMI-1 data archive (https://data.ceda.ac.uk/badc/wcrp-ccmi/data/CCMI-1). The SOCOLv3 data for 2014-2018 were produced using the CCM SOCOLv3 version used in CCMI-1.

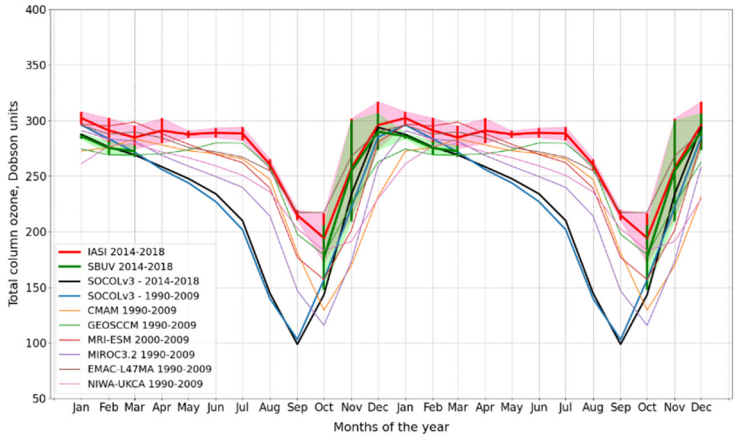

Figure 1. Annual course of TCO (DU) at 75-80S according to the satellite measurements with IASI and SBUV sensors and the results of SOCOLv3, CMAM, GEOSCCM, MRI-ESM, MIROC3.2, EMAC-L47MA, and NIWA-UKCA chemistry-climate models. The averaging periods are 2014-2018 for satellite data and SOCOLv3 and 1990-2009 for all other model data. Shaded areas represent the standard deviation of the data.

The figure demonstrates a good agreement between SBUV and IASI data during the austral spring and summer seasons (October-February) when the SBUV data are available. The comparison of the CCM SOCOLv3 data from 1990-2009 and 2014-2018 suggests weak changes in the TCO behavior during austral fall and wintertime. It is visible that all CCMs underestimate the polar TCO values from April to September. The GEOSCCM has the smallest deviation, while the SOCOLv3 shows the largest (~100 DU) error relative to IASI data. From October to December the SOCOLv3, GEOSCCM, MRI-ESM, and EMAC agree with the IASI data within the uncertainty range, while MIROC3.2, CMAM, and NIWA-UKCA demonstrate some underestimation. Therefore, the level of TCO in October, which is usually used for the evaluation of the model performance in the simulation of the ozone hole does not give full information about model quality. The polar night area is the most interesting point because virtually all models show smaller TCO in comparison with satellite data.

In this study, we try to understand and improve the representation of the southern polar TCO in the CCM SOCOLv3, as we have full access to this model. To solve the problem, we considered several factors affecting the annual cycle of polar ozone in the Southern Hemisphere: (1) the rates of the heterogeneous reactions; (2) photolysis rates of O_3 for the large solar zenith angles; (3) sub-grid-scale meridional mixing (into the polar vortexes).

A brief description of the IASI instrument characteristics, CCM SOCOLv3 modules and performed sensitivity runs are presented in Section 2. The obtained results are described and discussed in Sections 3 and 4 respectively. Section 5 contains the summary of the study and the main conclusions.

Preprints (www.preprints.org) | NOT PEER-REVIEWED | Posted: 20 September 2023 doi:10.20944/preprints202309.1348.v1

2. Materials and Methods

2.1. IASI sensor

IASI is an interferometer that measures the electromagnetic spectrum of the outgoing infrared radiation at a horizontal resolution of 12 km over a swath width of about 2,200km. With 14 orbits in a sun-synchronous mid-morning orbit (9:30 Local Solar Time equator crossing, descending node) global observations can be provided twice a day [10]. The process of optical interferometry makes it possible to obtain accurate emission spectra of the atmosphere in the infrared wavelength range from 3.4 to 15.5 micrometers. TCO is produced with a relative error of 5% and with a horizontal resolution typically 25 km. The data of the IASI instrument can be freely downloaded from the instrument site (https://iasi.aeris-data.fr/).

2.2. CCM SOCOLv3

The CCM SOCOLv3 interactively calculates dynamic processes, hydrological cycle, cloud formation, convection, solar and thermal radiation fluxes, photolysis, chemical transformations, and vertical and horizontal transport of species. The main components of the model are depicted in Figure 2.

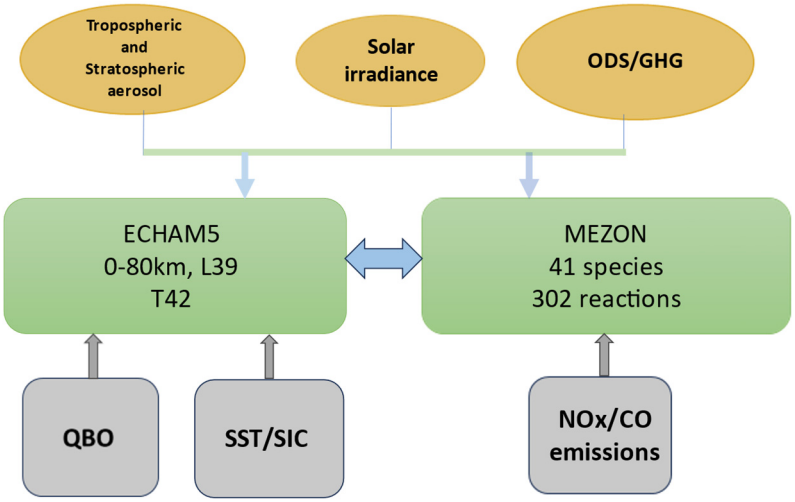

Figure 2. The main components of the CCM SOCOLv3.

The CCM SOCOLv3 consists of the general circulation model (GCM) of the middle atmosphere ECHAM5 and the chemical module (CM) MEZON. GCM and CM are interactively linked by 3D fields of temperature, winds (from GCM to CM), and radiatively active species such as water vapor, ozone, methane, nitrous oxide, and chlorofluorocarbons (from CM to GCM). The model includes 41 chemical elements from the groups of oxygen, hydrogen, nitrogen, carbon, chlorine, and bromine. Interactions between gas species are determined by 140 gas phase reactions, 46 photolysis reactions, and 16 heterogeneous reactions on liquid sulfate aerosols and solid particles of water ice and nitric acid trihydrate [11]. As external drivers of the atmospheric state, the model can use greenhouse gases and ozone-depleting substances mixing ratios, sea surface temperature (SST) and sea ice concentration (SIC), spectral solar radiation, sulfate aerosols properties, and some other parameters.

The SOCOLv3 has 39 vertical levels (from the surface up to 0.01 hPa) and has been used with horizontal resolution T42. The model can be run very efficiently in parallel mode.

The model performance was successfully evaluated in the framework of the International CCM Intercomparison project CCMI-1 [12]. A detailed description of SOCOLv3 can be found in [11].

 doi:10.20944/preprints202309.1348.v1

2.3. Description of the model runs

2.3.1. Reference run (RR)

To compare the CCM SOCOLv3 original calculation results with the IASI measurements we have undertaken a 19-year-long reference numerical experiment for the 2000-2018 period. The first 14 years (2000-2013) of the model calculations were considered as spin up. It is necessary for the adaptation of the chemical composition and dynamics of the model atmosphere to the specific boundary conditions. The last 5 years of the model experiment (2014-2018) were used for analysis and comparison with the correspondent IASI observations.

As boundary conditions, we considered the long-term (2000-2018) evolution of the ozone depletion substance (ODS), greenhouse gas concentrations GHG, sea surface temperature and sea ice concentration (SST/SIC), and zonal winds in the equatorial stratosphere (QBO). The mixing ratios of ODS in the lower troposphere evolved according to the World Meteorological Organization (WMO) data [13]. The atmospheric mixing ratios of the main GHG (CO_2, CH_4, and N_2O) are taken from [14] until 2014 and extended to 2018 following the IPCC SSP2-4.5 scenario [15].

The SST/SIC fields for the 21st century prescribed as monthly means are adopted from the HadISST1 dataset provided by the UK Met Office Hadley Centre [16]. The QBO is produced by a linear relaxation ("nudging") of the model zonal winds in the equatorial stratosphere to a time series of observed wind [17]. The nudging is used between 20° N and 20° S from 90 hPa up to 3 hPa. Within the QBO core domain (10° N–10° S, 50– 8 hPa) the relaxation time is uniformly set to 7 days; outside this region, the damping depends on latitude and altitude [18]. Also, the evolutions of the 11-year solar activity [19], stratospheric aerosol contents [20], and the surface CO and NOx emissions from CMIP6 input4MIPs databases for the historical period to 2014 and following RCP2-4.5 until 2018 [21] were applied in the model runs as boundary conditions.

Figure 3 illustrates the TCO calculated in the reference run of SOCOLv3 and the corresponding values of TCO obtained from IASI observations. The figure reveals that the model heavily underestimated the TCO values over the polar region of the SH against the satellite data. In August the difference can exceed 100 DU.

2.3.2. Sensitivity runs

The above-mentioned discrepancies probably can be explained by the poor model representations of the processes that are responsible for the polar ozone state. According to the modern scientific paradigm, the ozone content in the polar stratosphere is controlled mainly by the rates of the heterogeneous reactions and the photodissociation of ozone molecules by solar radiation at the large zenith angles of the Sun [22]. Also, the level of TCO inside the inner part of the SH polar night vortex can depend on the horizontal resolution of the model [23]. So, if the model grid is rather rough it makes sense to consider the transport of the model species into the polar night vortexes by the sub-grid scale motions.

Therefore, to investigate the causes of the TCO underestimation and find some reasonable refinement of the model results, we performed described in the Table 1 set of additional numerical runs with CCM SOCOLv3. All these model runs were designed exactly as the reference run (boundary conditions, spin-up, using the 2014-2018 years model results for comparison with the satellite data).

Preprints (www.preprints.org) | NOT PEER-REVIEWED | Posted: 20 September 2023 doi:10.20944/preprints202309.1348.v1

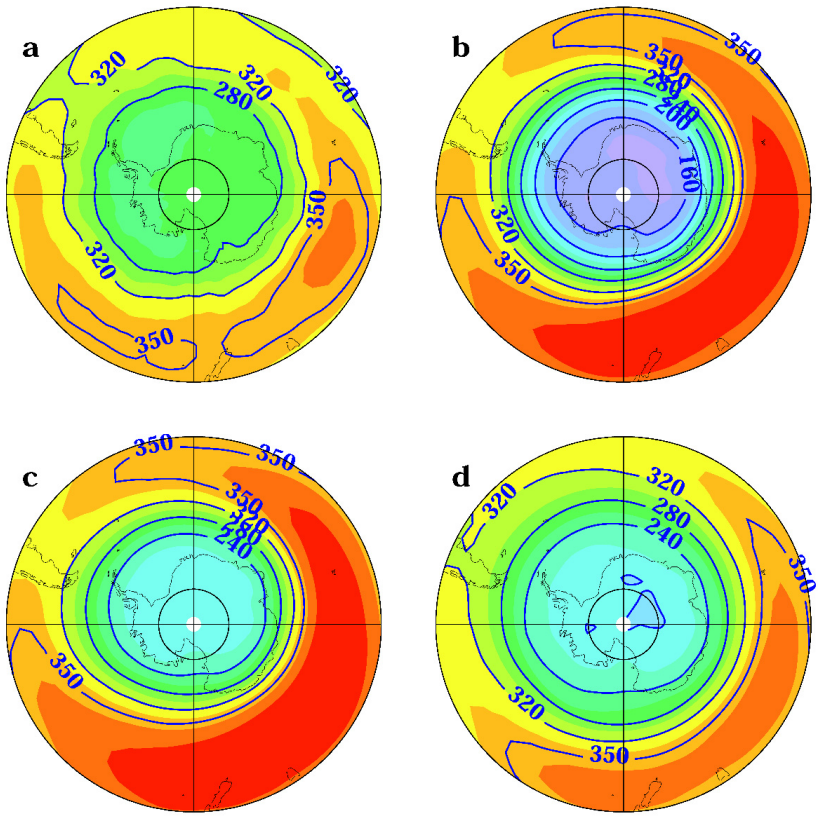

Figure 3. The TCO (DU) averaged over all Augusts during the 2014-2018 period from IASI data (**a**), reference run (**b**), SR2 run (**c**), and SR4 run (**d**).

Table 1. A short description of the sensitivity runs with CCM SOCOLv3.

Name of model run	Short description of the model run
SR1	The two times reduction of the heterogenies reaction HCl + $ClONO_2$ → Cl_2 + HNO_3 rate.
SR2	The four times reduction of the ozone photodissociation rates for the solar zenith angles ≥ 90^0
SR3	Including the horizontal mixing process of all transported model species into the SH polar vortex with diffusion coefficient $K_{yy} = 5 \cdot 10^6$ m^2/s in its maximum
SR4	SR2 + SR3

3. Results

3.1. Heterogeneous chemistry run (SR1)

Chemical reactions on/in polar stratospheric cloud particles play a crucial role in the formation of the Antarctic ozone hole [24], [Table 1]. To analyze the model TCO sensitivity to the intensity of heterogeneous processes we decreased by factor 2 the rate of the most important heterogeneous reaction HCl + $ClONO_2$ → Cl_2 + HNO_3, which provides the main source of the Cl_2 formation, which in turn produces active chlorines and destroys polar stratospheric ozone in the photo-catalytic cycle after polar sunrise.

Figure 4 shows the annul course of zonal/monthly mean TCO at 80^0S averaged from 2014 to 2018 years as the result of this experiment (green line) together with the correspondent values from the reference run (black line) and the IASI measurements (red line).

Preprints (www.preprints.org) | NOT PEER-REVIEWED | Posted: 20 September 2023 doi:10.20944/preprints202309.1348.v1

As expected, reduced efficiency of the $HCl + ClONO_2 \rightarrow Cl_2 + HNO_3$ reaction rate leads to weaker ozone depletion and higher TCO only from October to December. However, the rate correction does not affect the TCO values inside the polar vortex during the polar night and cannot improve the result of the model calculation of TCO against IASI observations.

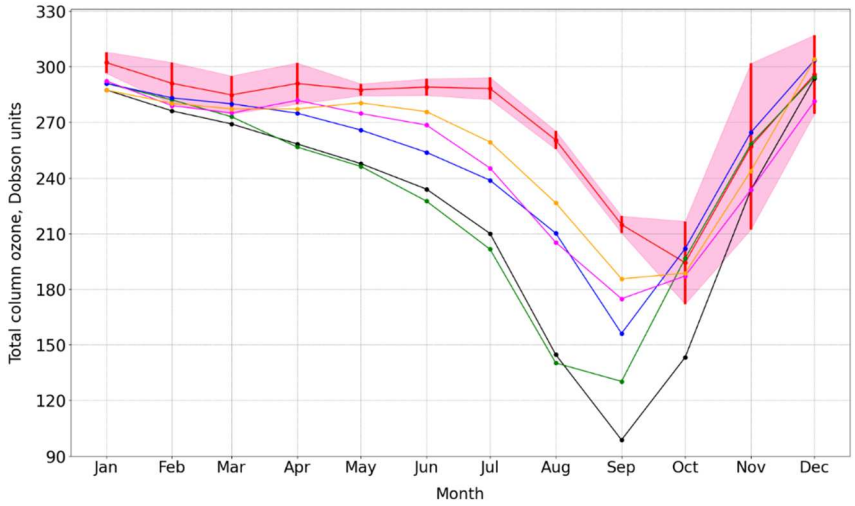

Figure 4. TCO (DU) averaged over 2014-2018, at the 80S as the IASI measurements (red) and the results of the reference (black), SR1 (green), SR2 (blue), SR3 (magenta), and SR4 (orange) experiments.

3.2. Reduced photodissociation of O_3 run (SR2)

To compute the photolysis rates in SOCOLv3 the lookup-table method (LUT) is used [25]. Also, in the case of large zenith angels of the Sun, spherical geometry is included in the model calculation of the photolyze rates. This approach provides the not-zero photodissociation values even when the solar zenith angle exceeds 90^o, but the accuracy of this addition to the LUT scheme was not qualified. It is known, however, from the natural balloon observations in the stratosphere [26] that the ozone concentration is almost insensitive to solar radiation when the zenith angels of the Sun > 90^0. Therefore, a suggestion was made, that the model photolysis rates of O_3 are overestimated at large solar zenith angles. According to this suggestion, we performed the model run with decreasing photolysis of O_3 by factor 4 when the solar zenith angle exceeded 90^o. Figure 3 depicts the TCO for the model run with reduced O_3 photodissociation rate (Figure 3c) and the appropriate IASI measurements (Figure 3a).

In this model run the concentration of $O(^3P)$ and $O(^1D)$ atoms decreases at the large solar zenith angles and as a result, the catalytic cycles of the ozone destruction are less effective [24], [Table 1]. As it is shown in Figure 4 it leads to much better agreement between the modeled and observed TCO inside the vortex area. This improvement, however, affects TCO amount in the middle and high latitudes from July to November and leads to TCO enhancement in comparison with IASI measurements (see Figure 3).

From these results, we conclude that the applied decrease of the ozone photolysis rate can solve the problem of the large deficit of ozone inside the polar vortex area, but deteriorate the model accuracy over the middle and high latitudes in the SH. The obtained results also suggest that this TCO bias in the model can be explained by the insufficient horizontal transport of ozone in the model from the middle latitudes to the region covered by the circumpolar vortex in the SH.

3.3. Model run with the subgrid-scale mixing (SR3)

Previous numerical experiments with the chemistry-transport models provided some evidence that the air mass exchange between the polar vortex area and the middle latitude in the SH stratosphere depends on the applied horizontal resolution [23,27]. The calculated mass fluxes into the inner region of the vortex from outside increase when the model's horizontal resolution is higher. It

Preprints (www.preprints.org) | NOT PEER-REVIEWED | Posted: 20 September 2023 doi:10.20944/preprints202309.1348.v1

can be explained by the fact that the model with the higher horizontal resolution generates additional transport by the atmospheric motions that cannot be resolved by the model with the coarse grid.

To verify this suggestion for SOCOLv3 we included in the model lower stratosphere a zonally averaged meridional diffusion of the species with a coefficient K_{yy} which depends only on time and latitude. According to the Prandl mixing length theory the maximum values of K_{yy} can be estimated as < $6 \cdot 10^6$ m^2/s (mixing length < $3 \cdot 10^5$ m and meridional wind variations < 20 m/s on the model meridional grid scale (~ 2.5^0)). We suggest also that the K_{yy} reached its maximum in the areas of the polar vortex locations. The time-latitudinal mask for the K_{yy} values is presented in Figure 5.

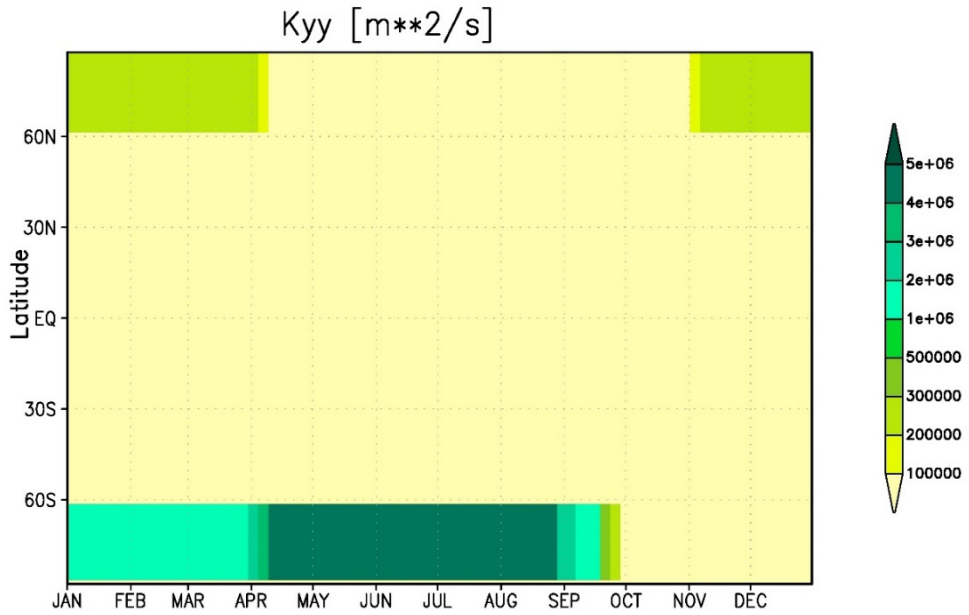

Figure 5. The time-latitudinal mask of K_{yy} value with maximum equals $5 \cdot 10^6$ m^2/s (SR3 and SR4 model runs).

To evaluate the sensitivity of the model calculations to the intensity of the suggested diffusion process a set of the model runs was undertaken with K_{yy} varying from $3 \cdot 10^5$ m^2/s to $6 \cdot 10^6$ m^2/s in its maximum. The most reasonable result was obtained in the run with the maximum value of $K_{yy} = 5 \cdot 10^6$ m^2/s (run SR3).

The zonal/monthly mean TCO for ~80^0S from SR3 together with the correspondent TCO data from the other runs and IASI observations are presented in Figure 4 which demonstrates that enhancement of the subgrid-scale mixing process in the model leads to a remarkable decrease in the TCO bias of CCM SOCOLv3 in comparison with the results of the satellite measurements. Therefore, it could be expected, that this very simplified approach can be useful for the CCMs with coarse horizontal grid (>1^0) and will be much less significant for the CCMs with much finer horizontal resolution.

3.4. Model run with extra mixing and weaker photolysis (SR4)

The SR2 (4-fold reduced photo-dissociations rate of O_3 (SAZ > 90^0)) and SR3 (subgrid-scale mixing with maximum $K_{yy} = 5 \cdot 10^6$ m^2/s) corrections allow us to improve the model representation of TCO in the polar region of the SH (see Figure 4). But even after the improvement the disagreement against the IASI observation is still high. For example, the TCO from the SR3 run still starts to decrease too early in comparison with the IASI observations—in May (see Figure 4). Also, the TCO difference between CCM SOCOLv3 and IASI is still substantial and is equal to approximately half the correspondent difference that was found in the reference experiment.

On the other hand, both corrections (SR2 and SR3) affect the TCO values independently and have some theoretical and experimental reasons [23,26,27]. Therefore, it is reasonable to perform the model run applying both improvements simultaneously (SR4 run = SR2 + SR3). The zonal/monthly

mean TCO for ~80^{0}S from the SR4 experiment together with the correspondent TCO values from the reference run and the IASI observations are presented in Figure 4. Figure 3d depicts the TCO values from the model SR4 run averaged over all Augusts during 2014-2018 in comparison with the correspondent IASI data (Figure 3a) in the SH.

Figures 3 and 4 show that the joint corrections applied in the SR4 experiment allow us to obtain the TCO patterns which are much closer to the IASI measurements than the correspondent results of SR2 and SR3 separately. So, in the SR4 run a substantial part of ozone is transported from the middle latitudes into the ozone hole area and destroyed there. As a result, the TCO overestimation in the middle latitudes of the SR2 run (Figure 5) disappeared during the polar night and after breaking the polar vortex.

Finally, from the comparison of the SR4 results against the reference run output (Figure 3), it can be found that the SR2 and SR3 corrections included in CCM SOCOLv3 have mainly resolved the problem of the very low model TCO values over the polar regions in the SH.

4. Discussion

Availability of the high-quality satellite measurements by IASI instrument has provided a powerful impulse for the evaluation of the CCMs performance over the polar regions, especially under polar night conditions. Comparison of the results of TCO modeling by the CCM SOCOv3 and other CCMs with the IASI satellite instrument data revealed the existence of too-low values of the model TCO during the polar night inside the southern vortex. To understand the potential causes of the problem, we studied with the CCM SOCOLv3 the sensitivity of the total column ozone over Antarctica to (1) photo-dissociation rates of ozone for large solar zenith angles; (2) rates of the stratospheric heterogeneous reactions under the polar night conditions and (3) intensity of the meridional mixing on the model sub-grid scales into the polar regions. Comparisons of the modeling results with the correspondent data of the IASI measurement showed that the most important characteristics for the improvement of the simulated polar ozone are photolysis for the large zenith angles and intensity of horizontal mixing into the polar vortexes. The applied tuning of these processes has allowed us to substantially improve the model representation of the ozone annual cycle over the polar regions reducing the model TCO difference against the IASI measurements from 100 to about 20 DU in August. The proposed increase of the horizontal mixing can be recommended for the CCMs with relatively low (more than 1 deg) horizontal resolution.

Author Contributions: Conceptualization, E.R., V.Z and T.A.; methodology V.Z. and E.R.; software, V.Z. and A.M.; formal analysis, V.Z, A.M., E. R. and T.A.; resources, E. R.; data curation, V.Z.; writing—original draft preparation, A.M.; writing—review and editing, V.Z, A.M., E. R. and T.A.; visualization, A.M., V.Z and E.R..; supervision, E.R.; project administration, E.R.; funding acquisition, E.R. All authors have read and agreed to the published version of the manuscript.

Funding: This research was funded by the Government of the Russian Federation grant (075-15-2021-583) to Saint Petersburg State University "Ozone Layer and Upper Atmosphere Research Laboratory".

Data Availability Statement: The datasets presented and discussed in this study can be found in online repositories https://doi.org/10.5281/zenodo.8341582.

Acknowledgments: Model simulations have been performed on the SPBU cluster. We acknowledge the help of A. Divin and A. Zarochentsev with the model maintenance and execution.

Conflicts of Interest: The authors declare no conflict of interest. The funders had no role in the design of the study; in the collection, analyses, or interpretation of data; in the writing of the manuscript; or in the decision to publish the results.

References

1. Bernhard, G.H., Neale, R.E., Barnes P. W., et al. Environmental effects of stratospheric ozone depletion, UV radiation and interactions with climate change: UNEP Environmental Effects Assessment Panel, update 2019, Photochem Photobiol Sci, 2020, 19, 542, https://doi.org/10.1039/d0pp90011g.
2. Farman, J., Gardiner, B. and Shanklin, J. Large losses of total ozone in Antarctica reveal seasonal ClO_x/NO_x interaction. Nature, 1985, 315, 207–210 https://doi.org/10.1038/315207a0.
3. Egorova, T., E. Rozanov, Gröbner, J., Hauser, M., and Schmutz, W. Montreal Protocol benefits simulated with CCM SOCOL, Atmos. Chem. Phys., 2013, 13, 3811–3823, doi:10.5194/acp-13-3811-2013.
4. SPARC, 2010: SPARC CCMVal Report on the Evaluation of Chemistry-Climate Models. V. Eyring, T. Shepherd and D. Waugh (Eds.), SPARC Report No. 5, WCRP-30/2010, WMO/TD – No. 40, available at www.sparc-climate.org/publications/sparc-reports/.
5. Eyring, V., Chipperfield, M., Giorgetta, M. et al. Overview of the New CCMVal Reference and Sensitivity Simulations in Support of Upcoming Ozone and Climate Assessments and the Planned SPARC CCMVal, SPARC Newsletter No. 30, 2008, 20–26, http://www.atmosp.physics.utoronto.ca/SPARC/Newsletter30Web/53294-1%20SPRAC%20Newsletter-LR.pdf.
6. Dhomse, S. S., Kinnison, D., Chipperfield, M. P. et al. Estimates of ozone return dates from Chemistry-Climate Model Initiative simulations, Atmos. Chem. Phys., 2018, 18, 8409–8438, https://doi.org/10.5194/acp-18-8409-2018.
7. Siddaway, J. M., Petelina, S. V., Karoly, D. J., Klekociuk, A. R., and Dargaville, R. J. Evolution of Antarctic ozone in September–December predicted by CCMVal-2 model simulations for the 21st century, Atmos. Chem. Phys., 2013, 13, 4413–4427, https://doi.org/10.5194/acp-13-4413-2013.
8. Karpechko, A. Y., Maraun, D., and Eyring V. Improving Antarctic total ozone projections by a process-oriented multiple diagnostic ensemble regression. J. Atmos. Sci., 70, 2013, 3959–3976, https://doi.org/10.1175/JAS-D-13-071.1.
9. Corlett, G. K., and Monks, P. S. A comparison of total ozone values derived from the Global Ozone Monitoring Experiment (GOME), the Tiros Operational Vertical Sounder (TOVS) and the Total Ozone Mapping Spectrometer (TOMS), J. Atmos. Sci., 2001, 58, 1103–1116, https://doi.org/10.1175/1520-0469(2001)058<1103:ACOTCO>2.0.CO;2.
10. Boynard, A., Hurtmans, D., Garane, K. et al. Validation of the IASI FORLI/EUMETSAT ozone products using satellite (GOME-2), ground-based (Brewer–Dobson, SAOZ, FTIR) and ozonesonde measurements, Atmos. Meas. Tech., 2018, 11, 5125–5152, https://doi.org/10.5194/amt-11-5125-2018.
11. Stenke, A., Schraner, M., Rozanov, E., Egorova, T., Luo, B., and Peter, T. The SOCOL version 3.0 chemistry–climate model: description, evaluation, and implications from an advanced transport algorithm, Geosci. Model Dev., 2013, 6, 1407–1427, https://doi.org/10.5194/gmd-6-1407-2013.
12. Hegglin, M.I.. Lamarque, J.F.. Eyring, V. The IGAC/SPARC Chemistry-Climate Model Initiative Phase-1 (CCMI-1) model data output. NCAS British Atmospheric Data Centre, 2015, http://catalogue.ceda.ac.uk/uuid/9cc6b94df0f4469d8066d69b5df879d5.
13. WMO (World Meteorological Organization), Scientific Assessment of Ozone Depletion: 2018, Global Ozone Research and Monitoring Project–Report No. 58, 588 pp., Geneva, Switzerland, 2018.
14. Meinshausen, M., Vogel, E., Nauels, A. et al. Historical greenhouse gas concentrations for climate modelling (CMIP6), Geosci. Model Dev., 2017, 10, 2057-2116, https://doi.org/10.5194/gmd-10-2057-2017.
15. Meinshausen, M., Nicholls, Z. R. J., Lewis, J. et al. The shared socio-economic pathway (SSP) greenhouse gas concentrations and their extensions to 2500, Geosci. Model Dev., 2020, 13, 3571–3605, https://doi.org/10.5194/gmd-13-3571-2020.
16. Rayner, N. A., Parker, D. E., Horton, E. B., et al. Global analyses of sea surface temperature, sea ice, and night marine air temperature since the late nineteenth century. J. Geoph.Res.:Atmospheres, 2003, 108, https://doi.org/10.1029/2002JD002670.
17. Giorgetta, M. A.: Der Einfluss der quasi-zweijahrigen Oszillation: ¨ Modellrechnungen mit ECHAM4, Max-Planck-Institut fur Meteorologie", Hamburg, Examensarbeit Nr. 40, MPI-Report 218, 1996.
18. Giorgetta, M. A., Manzini, E., Roeckner, E., Esch, M., and Bengtsson, L. Climatology and forcing of the quasi-biennial oscillation in the MAECHAM5 model, J. Climate, 2006, 19, 3882–3901, https://doi.org/10.1175/JCLI3830.1.
19. Matthes, K., Funke, B., Anderson, M. E. et al. Solar Forcing for CMIP6 (v3.2). Geosci. Model Dev.,2017, 10, https://doi.org/10.5194/gmd-10-2247-2017.

20. Kovilakam, M., Thomason, L. W., Ernest, N., Rieger, L., Bourassa, A., and Millán, L. The Global Space-based Stratospheric Aerosol Climatology (version 2.0): 1979–2018, Earth Syst. Sci. Data, 2020, 12, 2607–2634, https://doi.org/10.5194/essd-12-2607-2020.
21. Hoesly, R. M., Smith, S. J., Feng, L. et al. Historical (1750-2014) anthropogenic emissions of reactive gases and aerosols from the Community Emissions Data System (CEDS), Geosci. Model Dev., 2018, 11, 369–408, https://doi.org/10.5194/gmd-11-369-2018.
22. Brasseur, G. and Solomon, S.: Aeronomy of the Middle Atmosphere: Chemistry and Physics of the Stratosphere and Mesosphere, Atmospheric and Oceanographic Sciences Library, Springer Netherlands, https://books.google.nl/books?id=HoV1VNFJwVwC, 2005.
23. Shuhua L., Cordero, E., and Karoly, D. Transport out of the Antarctic polar vortex from a three-dimensional transport model, J. Geophys. Res., 2002, 107, https://doi.org/10.1029/2001JD000508.
24. Solomon, S.: Stratospheric ozone depletion: A review of concepts and history, Rev. Geophys., 1999, 37, 275–316, https://doi.org/10.1029/1999RG900008
25. Rozanov, E., Zubov, V., Schlesinger, M., Yang, F., and Andronova, N. The UIUC 3-D Stratospheric Chemical Transport Model: Description and Evaluation of the Simulated Source Gases and Ozone, J. Geophys. Res., 1999, 104, 11755-11781, https://doi.org/10.1029/1999JD900138.
26. Sheldon, W.R., Benbrook' J. R., and Aimedieu, P. Ozone depletion in the upper stratosphere at the dawn terminator, JASTP, 1997, 59, 1-7, https://doi.org/10.1016/S1364-6826(96)00055-7.
27. Wauben, W. M. F., Bintanja, R., van Velthoven, P. F. J., and Kelder H. M. On the magnitude of transport out of the Antarctic polar vortex, J. Geophys. Res., 1997, 102, 1229 – 1238, https://doi.org/10.1029/96JD02741.